(Received 22 October 2024, Accepted 13 December 2024, Scheduled 8 January 2025)

Petal-Shaped Array Antenna with Slots for Improving Surface Current Distribution

Jia-Feng Zhou and Jiu-Sheng Li*

Center for THz Research, China Jiliang University, Hangzhou 310018, China

ABSTRACT: To improve surface current distribution and give dual polarizations, a petal-shaped array antenna with slots was presented. We analyze the surface current of petal-shaped array antenna, study the working modes of each part, and use defect structures to remove surface reverse currents to reduce sidelobes and achieve high gain characteristics. By changing the radiation length of the antenna, the designed antenna operates in the target frequency band. Then, strip defects are introduced to improve surface current and enhance isolation. Finally, antenna prototype was fabricated and measured to demonstrate our ideas. The measured results show that the proposed antenna has a 10 dB impedance bandwidth from 5.74 to 5.82 GHz with a relative bandwidth of 1.4% and achieves a peak gain of 11.3 dBi at 5.8 GHz. The isolation of the two ports is more than 26.4 dB in the passband. The overall size of the proposed antenna is only $1.47\lambda_0 \times 1.47\lambda_0 \times 0.015\lambda_0$.

1. INTRODUCTION

As a novel antenna technology, dual-polarized antennas exhibit superior performance in the suppression of multipath fading, enhancement of channel capacity and spectral efficiency. Its most prominent advantage is that it can save the number of antennas for a single directional base station. Consequently, dual-polarized antennas are highly competitive in communication systems [1]. Under various requirements, some literature has explored different types of dual polarized antennas, such as dielectric resonant antennas [2, 3], dipole antennas [4–6], slots [7], and microstrip antennas [8, 9]. Among them, microstrip antennas are the most prevalent type employed in contemporary wireless systems, due to their numerous advantages such as low profile, low cost, and compatibility with planar circuits. Given that antenna gain has a direct impact on system performance, various techniques have been proposed to enhance the gain of antennas such as slotted patch antennas [10] and introduction of new resonant modes [11, 12]. In [11], broadband performance is achieved by combining the quasi TM30 mode introduced by a mushroom-shaped structure and the original TM10 mode generated by the main radiating patch. In [13], a new wideband near-field probing antenna was proposed to increase the effective isotropic radiated power from 32 dBm to 34.1 dBm. It is evident that antenna arrays can effectively enhance the gain, as evidenced by [14]. However, the size of the array antenna is typically considerable, and the feed network can complicate the overall system structure.

The antenna's dual-polarization characteristics are generally achieved by dual-port feeding, and the isolation between ports is also an important parameter to measure the performance of dual-polarized antennas. Various methods to improve port isolation have been studied in the literature such as dedicated feed network [15], vias feed [16], frequency selective surface [17], polarized isolation cavity [18], concurrent dual-mode substrate integrated waveguide structure [19], and stacked patches [20]. Designing a dedicated feed network can directly and effectively improve the port isolation, and differential feeding can effectively excite two polarization modes to improve the port isolation [15]. In [16], the use of vias to feed each part of the antenna individually can effectively reduce surface waves to achieve very good isolation. In addition, in [18], the use of a polarized isolation cavity makes the isolation degree much higher than 50 dB; however, it makes the overall structure of the antenna very complicated. Overall, it is still quite challenging to design dual-polarized microstrip antennas with high gain and high isolation.

In this paper, a petal-shaped microstrip patch antenna is investigated. The surface current and operating mode of the antenna are analyzed, and the central reverse current portion of the patch is removed to suppress the sidelope level. The operating band is adjusted by changing the equivalent electrical length, and the slot defects are added to improve the antenna isolation. Finally, a dual-polarized microstrip patch antenna is fabricated and measured to verify the correction effect of the proposed method. The proposed antenna exhibits promising usage in diversity and MIMO systems.

2. ANTENNA DESIGN

2.1. Antenna Configuration

Figure 1 illustrates the general pattern and detailed dimensions of the designed antenna. The antenna consists of four circular patches arranged in a conventional petal-shape with a circular defect in the center of the antenna, an inward-facing semicircular protrusion within the defect near each of the two feed points, and an outward-facing bar notch on the patch between the two feed points. The antenna is printed on an F4BME220 dielec-

* Corresponding author: Jiu-Sheng Li (jshli@126.com).

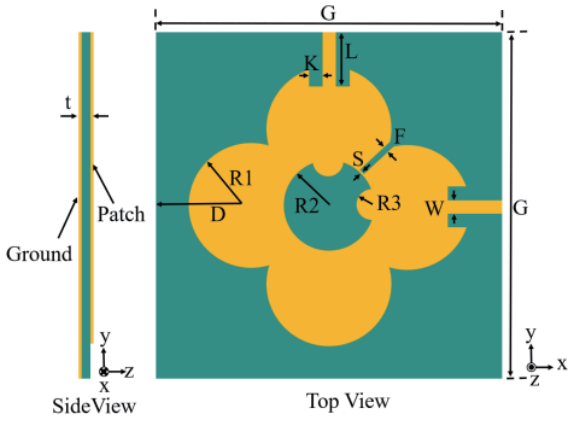

FIGURE 1. Configuration of the proposed antenna: $D = 21$, $F = 1$, $G = 76$, $L = 11.8$, $K = 3$, $R1 = 13.8$, $R2 = 10$, $R3 = 3.3$, $S = 0.5$, $W = 3$, and $t = 0.762$ (unit: mm).

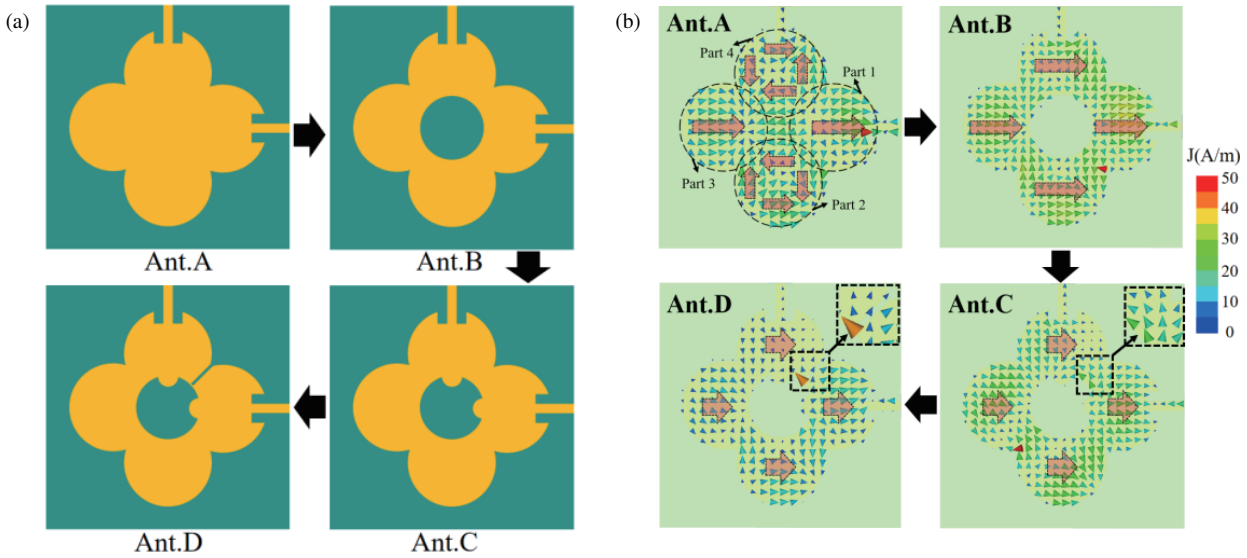

FIGURE 2. (a) The evolution process of the petal-shaped array antenna. (b) Current distributions of the antenna evolution at resonant frequency.

tric substrate ($\varepsilon_r = 2.2$, $\tan\delta = 0.0007$) with a thickness of $t = 0.762$ mm. Two 50Ω SMAs are used to excite each polarization of the antenna. The interior part of the 50 Ω SMA is linked to the patch by means of a 50 Ω microstrip line, while the exterior part is welded to the ground plane. The signal source is usually connected through a 50 Ω SMA connector, and the impedance of the antenna's feed line is set to 50 Ω. Based on the dielectric constant, loss tangent parameter, and thickness of the substrate, we can use a Commercial software to obtain the microstrip line width corresponding to an impedance of 50 Ω. The length of the microstrip line only affects the phase of the input signal, while the distance between the edge of the antenna patch and the edge of the board is generally set to $\lambda/4$, and the length of the feeder can be adjusted appropriately according to $\lambda/4$.

2.2. Operating Principle

To achieve high gain and high isolation, a dual-polarized antenna is proposed to improve the antenna surface current by using defective structures and by changing the antenna operating mode. Two feed lines are arranged vertically to achieve dual polarizations. The evolution process of the petal-shaped array antenna (marked as Ant. A, Ant. B, Ant. C, Ant. D) is shown in Fig. 2(a). The simulation current distribution of the antenna evolution is shown in Fig. 2(b). Obviously, Part 1 and Part 3 in Ant. A operate in TM_{11} mode, while Part 2 and Part 4 operate in TM_{21} mode. It can be noted that the inverted phase currents of the high order modes generate side interference. From the figure, one can see that the current in the center part of Ant. A is anti-phase compared with that of the other parts. From Fig. 2(b), it can be observed that the anti-phase current can be eliminated by digging a hole in the center part of Ant. A (Marked as Ant. B). At this time, the surface current distribution in the four parts of the proposed antenna keeps the same direction, which makes more energy to concentrate on the main flap (see Fig. 3). The paraflap level increases from −13.1 dB to −20.2 dB.

The effect of various D (i.e., spacing between the center of the circular patches and the edge of the substrate) on the di-

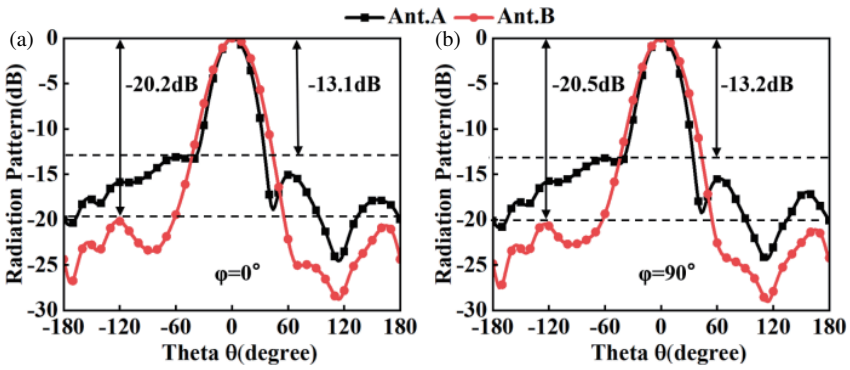

FIGURE 3. Radiation patterns of Ant. A and Ant. B in different plane. (a) $\varphi = 0°$, (b) $\varphi = 90°$.

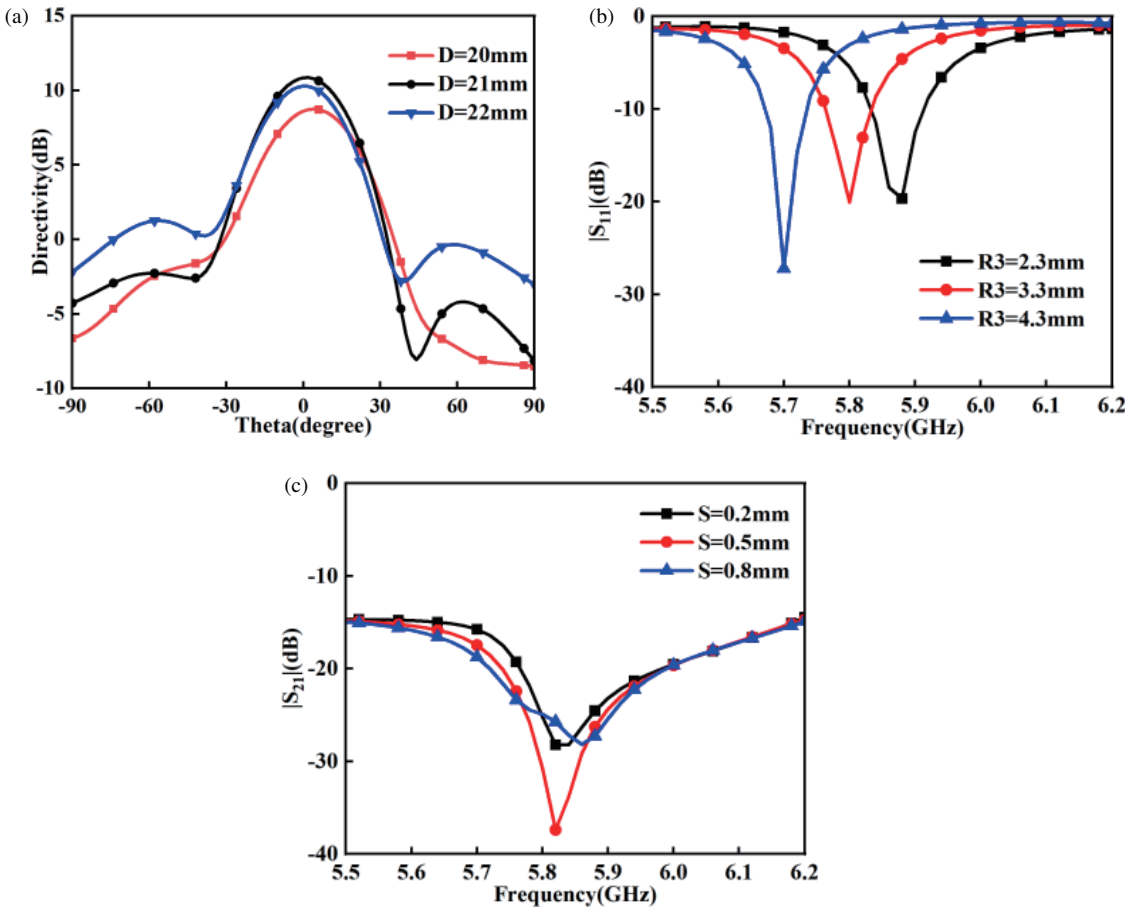

FIGURE 4. (a) Directivity of the Ant. D with various D, (b) S_{11} versus different $R3$, (c) S_{21} versus different S.

rectivity is given in Fig. 4(a). We can find that the maximum directivity of Ant. D is 10.85 dB when $D = 21$ mm. From Fig. 4(b), it is found that the size of the semi-circular patch has a significant effect on the resonance frequency of the antenna resonance frequency. When $R3 = 3.3$ mm, the operating frequency is 5.8 GHz, which is consistent with expected results. Fig. 4(c) shows the effect of the rectangular defect depth on the $|S_{21}|$ parameters of the antenna. It can be clearly seen that when $S = 0.5$ mm, the isolation of the antenna is the best. The $S_{11(22)}$ evolution performances of the proposed antennas are shown in Fig. 5(a). The resonance frequency of Ant. D is 5.8 GHz, and the -10 dB bandwidth is 0.08 GHz (5.76–5.84 GHz). The antenna is fed by dual ports, and the S-parameters of the two ports (S_{11}, S_{22}) are kept the same due to the symmetrical structure. The isolation $|S_{21}|$ of Ant. D in the operating band is less than -25.8 dB, and the isolation is -37.4 dB at 5.82 GHz, as displayed in Fig. 5(b). Obviously, the addition of rectangular defect reduces the current interactions between the ports and does not have a visible impact on the antenna resonant frequency and gain, while improving the isolation between the dual ports. From Fig. 5(c), one can see that the gain of Ant. D is 12.1 dBi. When both ports are fed simultaneously, and the phase differ-

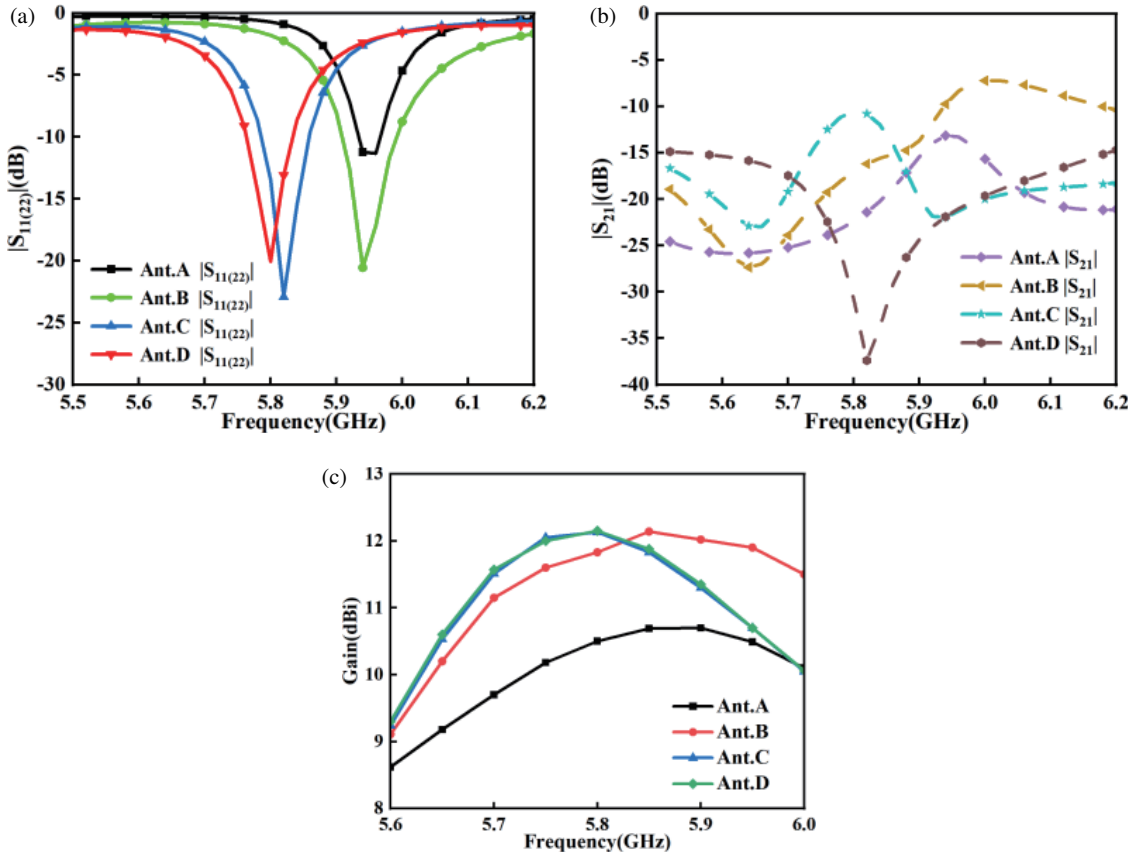

FIGURE 5. Simulated performance of the proposed antenna. (a) $S_{11(22)}$, (b) S_{21}, (c) Antenna gains.

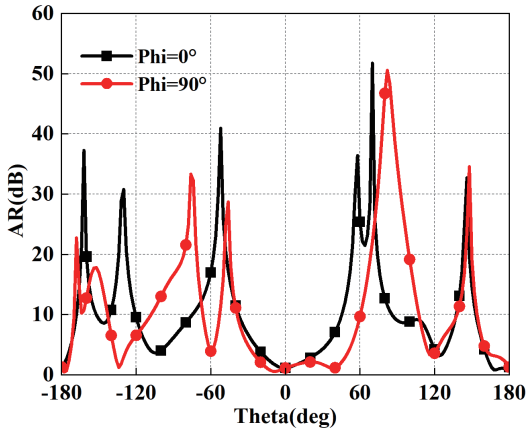

FIGURE 6. The axial direction of the antenna under both ports fed simultaneously.

ence is 90°, the axial direction of the antenna is shown in Fig. 6. When $Phi = 0°$, the axial ratio is less than 3 within the range of $-16°$ to 21°. When $Phi = 90°$, the axial ratio is less than 3 within the range of $-24°$ to 49°. It is indicated that the designed antenna can generate circularly polarized waves.

3. EXPERIMENTAL RESULTS

To verify the radiation characteristics of the proposed antenna, a prototype has been fabricated, and the top and bottom views of the fabricated prototype are shown in Figs. 7(a) and (b). Fig. 7(c) illustrates the measurement setup of the proposed antenna. As shown in Fig. 8(a), it can be observed that the measured reflection coefficients $|S_{11(22)}|$ of the two ports are less than -10 dB at 5.74–5.82 GHz and 5.74–5.81 GHz, with the bandwidths of 1.38% and 1.3%, respectively, which are in good agreement with the simulated results. The measured isolation between the two ports is larger than 25 dB within the operating bandwidth and reaches 30 dB at 5.8 GHz. The measured isolation between the two feed ports is almost identical to that of the simulated result. The simulated and measured gains of the dual-polarized antenna are shown in Fig. 8(b). When port 1 is excited, the gain at 5.8 GHz reaches 11.3 dBi with a radiation efficiency of 86.1%. While port 2 is excited, the peak gain achieves 10.9 dBi at 5.8 GHz with a radiation efficiency of 82.6%. Fig. 8(c) shows the envelope correlation coefficient (ECC), indicating that the ECC of our antenna is less than 0.39. Therefore, the designed antenna has broad application prospects with multiple input multiple output (MIMO) technology.

The simulated and measured normalized copolarized radiation patterns plots at 5.8 GHz are shown in Fig. 9. In our test, the antenna gives vertical polarization (co-polarization), then horizontal polarization is the cross polarization. The measured co-polarization (E_θ) levels are essentially consistent with those of the simulated results. The measured cross-polarization (E_φ) in the XOZ and YOZ planes is 20 dB lower than the copolarization. The small discrepancy between the simulated and

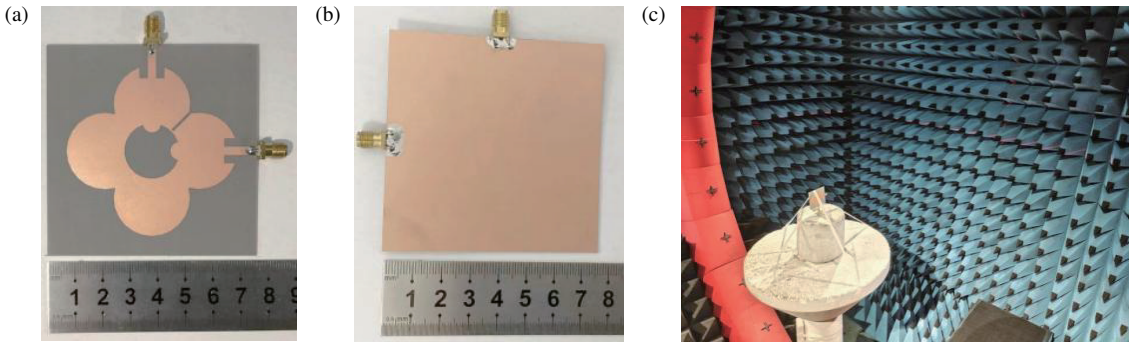

FIGURE 7. (a) Top view; (b) bottom view and (c) measurement setup of the fabricated prototype antenna.

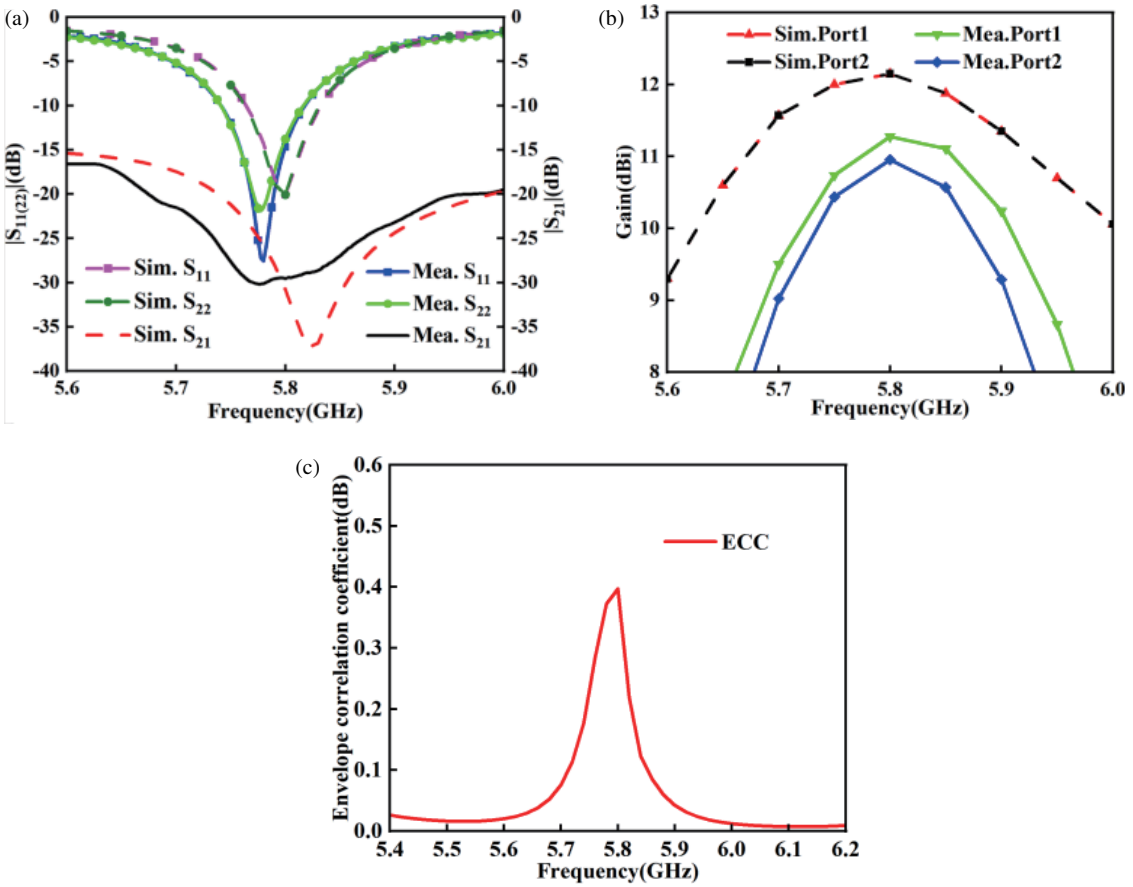

FIGURE 8. The measured results of the Ant. D. (a) S-parameter. (b) Antenna gain. (c) ECC.

TABLE 1. Comparison with the previous patch antennas.

Ref.	Frequency (GHz)	Gain (dBi)	Total size (λ^3)	Isolation (dB)
12	4.9	9.6	$1.3 \times 1.3 \times 0.49$	30
16	5.8	3.9	$0.96 \times 0.96 \times 0.03$	26.5
21	3.4/4.3	5.35/6.75	$1.0 \times 0.8 \times 0.018$	23
22	8.20/10.55	4.0/4.3	$0.6 \times 1.23 \times 0.027$	25
23	2.45/3.5	3.5/3.15	$0.48 \times 0.4 \times 0.013$	33
This work	5.8	11.3	$1.47 \times 1.47 \times 0.015$	30

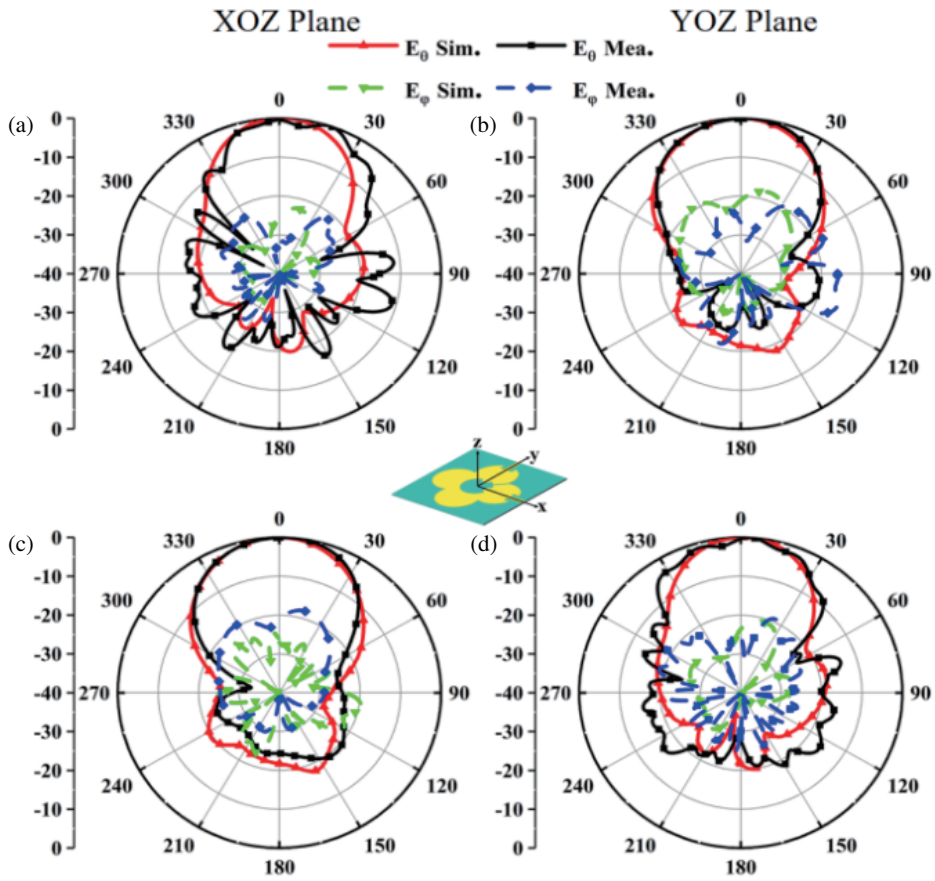

FIGURE 9. Simulated and measured radiation patterns of the proposed antenna fed through. (a) Port 1 in xoz plane. (b) Port 1 in yoz plane. (c) Port 2 in xoz plane. (d) Port 2 in yoz plane at 5.8 GHz.

experimental results is due to manufacturing and testing errors. A comprehensive comparison between our design and other dual-polarized patch antennas is presented in Table 1. The gain of our antenna is larger than that of the reported antennas in [12, 16, 21–23], and the isolation of the designed antenna is also excellent. Obviously, the proposed antenna has the advantages of high gain, good isolation, small size, compatibility with dual polarized applications, and simple structure.

4. CONCLUSION

We have proposed a petal-shaped array antenna with slots for improving surface current distribution and giving dual polarization. The petal-shaped antenna composed of circular patches achieves high gain after removing the central reverse current part, and the added small semi-circular patch regulates the resonant frequency of the antenna. By etching the strip-shaped groove, the isolation between the two ports has been significantly improved. Finally, a prototype was fabricated and measured to justify the correction of our idea. The proposed antenna has a 10 dB impedance bandwidth of 5.74 to 5.82 GHz, a relative bandwidth of 1.4%, and a peak gain of 10.67 dBi at 5.8 GHz. The measured isolation between the two ports reaches 30 dB at 5.8 GHz.

ACKNOWLEDGEMENT

This work was supported in part by the National Natural Science Foundation of China under Grant 62271460, Zhejiang Key R & D Project of China under Grant 2022C03166.

REFERENCES

[1] Jensen, M. A. and J. W. Wallace, "A review of antennas and propagation for MIMO wireless communications," *IEEE Transactions on Antennas and Propagation*, Vol. 52, No. 11, 2810–2824, Nov. 2004.

[2] Pan, Y. M., P. F. Hu, K. W. Leung, and X. Y. Zhang, "Compact single-/dual-polarized filtering dielectric resonator antennas," *IEEE Transactions on Antennas and Propagation*, Vol. 66, No. 9, 4474–4484, Sep. 2018.

[3] Tang, H., C. Tong, and J.-X. Chen, "Differential dual-polarized filtering dielectric resonator antenna," *IEEE Transactions on Antennas and Propagation*, Vol. 66, No. 8, 4298–4302, Aug. 2018.

[4] Wang, D., G. Wang, D. Lu, N. Yang, and Q. Zhang, "Design of wideband base station antenna by involving fragment-type structures on dipole arms," *IEEE Transactions on Antennas and Propagation*, Vol. 70, No. 7, 5953–5958, Jul. 2022.

[5] Yang, H., G. Zhao, J. Jiang, T. Liu, L. Zhao, Y. Li, Y. Cai, and J. Yao, "Aperture reduction using downward and upward bending arms for dual-polarized quadruple-folded-dipole antennas," *IEEE Antennas and Wireless Propagation Letters*, Vol. 22, No. 3,

645–649, Mar. 2023.

[6] Zhou, S.-G., Z.-H. Peng, G.-L. Huang, and C.-Y.-D. Sim, "Design of a novel wideband and dual-polarized magnetoelectric dipole antenna," *IEEE Transactions on Antennas and Propagation*, Vol. 65, No. 5, 2645–2649, Mar. 2017.

[7] He, Y., Y. Li, W. Sun, Z. Zhang, and P.-Y. Chen, "Dual linearly polarized microstrip antenna using a slot-loaded TM50 mode," *IEEE Antennas and Wireless Propagation Letters*, Vol. 17, No. 12, 2344–2348, Dec. 2018.

[8] Li, Y., Z. Zhao, Z. Tang, and Y. Yin, "Differentially fed, dual-band dual-polarized filtering antenna with high selectivity for 5G sub-6 GHz base station applications," *IEEE Transactions on Antennas and Propagation*, Vol. 68, No. 4, 3231–3236, Apr. 2020.

[9] Afshani, A. and K. Wu, "Dual-polarized patch antenna excited concurrently by a dual-mode substrate integrated waveguide," *IEEE Transactions on Antennas and Propagation*, Vol. 70, No. 3, 2322–2327, Mar. 2022.

[10] Hao, S.-S., Q.-Q. Chen, J.-Y. Li, and J. Xie, "A high-gain circularly polarized slotted patch antenna," *IEEE Antennas and Wireless Propagation Letters*, Vol. 19, No. 6, 1022–1026, Jun. 2020.

[11] Cao, Y., Y. Cai, W. Cao, B. Xi, Z. Qian, T. Wu, and L. Zhu, "Broadband and high-gain microstrip patch antenna loaded with parasitic mushroom-type structure," *IEEE Antennas and Wireless Propagation Letters*, Vol. 18, No. 7, 1405–1409, Jul. 2019.

[12] Luo, Y., Z. N. Chen, and K. Ma, "A single-layer dual-polarized differentially fed patch antenna with enhanced gain and bandwidth operating at dual compressed high-order modes using characteristic mode analysis," *IEEE Transactions on Antennas and Propagation*, Vol. 68, No. 5, 4082–4087, May 2020.

[13] Jin, H., A. B. Ayed, Z. He, B. Tung, and S. Boumaiza, "Embedded near-field probing antenna for enhancing the performance of 37-41-GHz linear and dual-polarized phased antenna arrays," *IEEE Microwave and Wireless Technology Letters*, Vol. 33, No. 6, 911–914, Jun. 2023.

[14] Jia, F., S. Liao, and Q. Xue, "A dual-band dual-polarized antenna array arrangement and its application for base station antennas," *IEEE Antennas and Wireless Propagation Letters*, Vol. 19, No. 6, 972–976, Jun. 2020.

[15] Zhang, X.-K., Y.-H. Ke, X.-Y. Wang, S.-C. Tang, and J.-X. Chen, "Broadband dual-polarized dielectric patch antenna with high isolation for full-duplex communication," *IEEE Antennas and Wireless Propagation Letters*, Vol. 22, No. 4, 878–882, Apr. 2023.

[16] Mirhadi, S., "Single-layer, dual-port, and dual-mode antenna with high isolation for WBAN communications," *IEEE Antennas and Wireless Propagation Letters*, Vol. 21, No. 3, 531–535, Mar. 2022.

[17] Ren, J., Z. Wang, Y.-X. Sun, R. Huang, and Y. Yin, "Ku/Ka-band dual-frequency shared-aperture antenna array with high isolation using frequency selective surface," *IEEE Antennas and Wireless Propagation Letters*, Vol. 22, No. 7, 1736–1740, Jul. 2023.

[18] Cheng, Y. J., F. Y. Tan, M. M. Zhou, and Y. Fan, "Dual-polarized wideband plate array antenna with high polarization isolation and low cross polarization for D-band high-capacity wireless application," *IEEE Antennas and Wireless Propagation Letters*, Vol. 19, No. 12, 2023–2027, Dec. 2020.

[19] Afshani, A. and K. Wu, "Dual-polarized patch antenna excited concurrently by a dual-mode substrate integrated waveguide," *IEEE Transactions on Antennas and Propagation*, Vol. 70, No. 3, 2322–2327, Mar. 2022.

[20] Wang, K., X. Liang, W. Zhu, J. Geng, J. Li, Z. Ding, and R. Jin, "A dual-wideband dual-polarized aperture-shared patch antenna with high isolation," *IEEE Antennas and Wireless Propagation Letters*, Vol. 17, No. 5, 735–738, May 2018.

[21] Pramodini, B., D. Chaturvedi, and G. Rana, "Design and investigation of dual-band 2×2 elements MIMO antenna-diplexer based on half-mode SIW," *IEEE Access*, Vol. 10, 79 272–79 280, 2022.

[22] Kumar, A. and S. Raghavan, "Planar cavity-backed self-diplexing antenna using two-layered structure," *Progress In Electromagnetics Research Letters*, Vol. 76, 91–96, 2018.

[23] Chaturvedi, D. and A. Kumar, "A QMSIW cavity-backed self-diplexing antenna with tunable resonant frequency using CSRR slot," *IEEE Antennas and Wireless Propagation Letters*, Vol. 23, No. 1, 259–263, Jan. 2024.